

## Compensation of Strand Magnetization in Superconducting Rutherford Cables Using Thin Iron Core

V.V. Kashikhin, A.V. Zlobin  
Fermilab, P.O. Box 500, Batavia, IL 60510

*Abstract* – The results of study of compensation technique of the coil magnetization effect in Nb3Sn high field dipole magnets in-situ using cables with thin ferromagnetic (iron) core are reported.

### 1. INTRODUCTION

A method of correction of the coil magnetization effect by ferromagnetic strips, placed inside the magnet bore is described in [1-2]. As it was shown, the ferromagnetic strips have rather good correction capability: 100-200  $\mu\text{m}$  thick 2-3 mm wide strips provide significant reduction of the induced sextupole at low fields. In this approach the source of correction effect (strips) is separated from the source of magnetization effect (superconductor) by the significant distance ( $\sim 1/2$  coil width).

Another possibility is to combine these two sources or, in the other words, to compensate the magnetization of superconducting strands by the magnetization of opposite sign generated by some magnetic material placed in the coil. In terms of compensation effect the best result can be achieved by distributing equally the compensating material inside the superconducting strands. For instance, the compensating magnetic material can be placed at strand surface as a thin film using electroplating or sputtering techniques. It can be also implemented inside the cable as a core between two layers of strands or can be wrapped around the cable. Additional positive effect of using a foil inside the cable (or coating strands) is a reduction of interstrand coupling currents since most of ferromagnetic materials have much higher resistance than copper. This type of compensation of the coil magnetization effect in Nb3Sn high field accelerator magnets is analyzed in this note.

### 2. AMOUNT OF FERROMAGNETIC MATERIAL

Let us find the amount of ferromagnetic material to be put inside the cable with bare area  $S_{cable}$  to reduce the magnetization of superconducting strand. A flux density in the material can be expressed in terms of field strength and magnetization as follows

$$\vec{B} = \mu_0 \cdot \vec{H} + \vec{M} \quad (1)$$

Let us assume the cable made of strands with a magnetization per strand  $M_{sc}(H)$  and packing factor of strands in the cable  $K_{sc}$ . Let us then consider a ferromagnetic material with magnetization  $M_{fe}(H)$  and packing factor  $K_{fe}$ , which is equally distributed within the cable. The cable area and the strand packing factor are remaining unchanged. In the case when vectors  $\vec{M}$  and  $\vec{H}$  are collinear the total flux density inside the cable is

$$B(H) = \mu_0 \cdot H + K_{sc} \cdot M_{sc}(H) + K_{fe} \cdot M_{fe}(H) \quad (2)$$

Since  $M_{sc}(H)$  and  $M_{fe}(H)$  are different functions of magnetic field the full compensation could be provided only at some reference field  $H_{ref}$ . Thus the flux density at  $H_{ref}$  in the superconducting cable with ferromagnetic strip inside is equal to the flux density of air

$$B(H_{ref}) = \mu_0 \cdot H_{ref} \quad (3)$$

Subtracting (3) from (2) at  $H_{ref}$  one can find the packing factor of ferromagnetic material inside the cable

$$K_{fe} = K_{sc} \cdot \frac{M_{sc}(H_{ref})}{M_{fe}(H_{ref})} \quad (4)$$

For the Nb3Sn (IGC) strand with  $J_c(12T)=1600 \text{ A/mm}^2$  and  $d_{eff}=100 \text{ }\mu\text{m}$ , the reference field  $\mu_0 H_{ref}=2.0 \text{ T}$  at which  $M_{sc}=-0.073 \text{ T}$ , the ferromagnetic material with saturation magnetization of 2.12 T and the cable packing factor of  $K_{sc}=0.88$  the packing factor of ferromagnetic material within the cable is  $K_{fe}=0.88 \cdot 0.073 / 2.12 = 0.03$  or only 3.0%. The integral magnetization curves for superconducting strand and ferromagnetic material after applying of the relevant packing factors are shown in Figure 1.

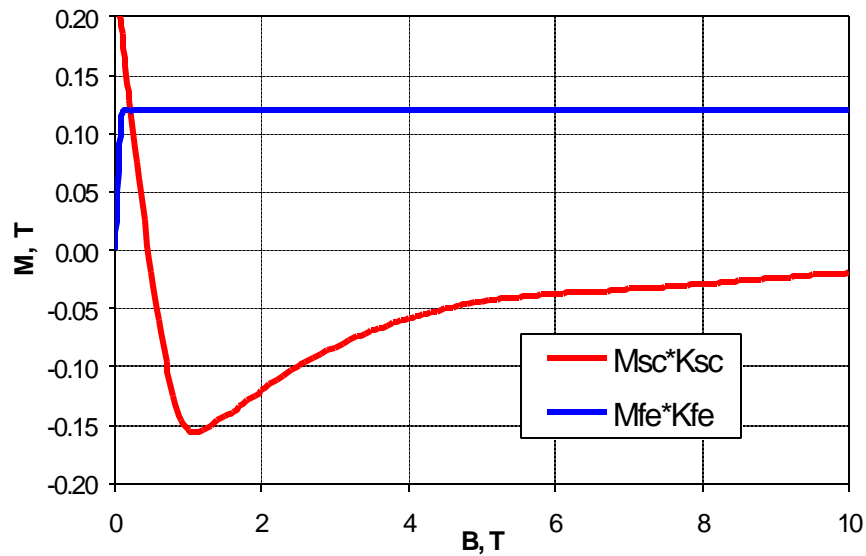


Figure 1: Magnetization of superconducting cable and ferromagnetic strips.

If the cable consists of  $N$  strands with the diameter of  $D_{strand}$ , and the ferromagnetic material is applied as strand coating, the thickness of such coating is:

$$\Delta_{fe} = \frac{\sqrt{\frac{4 \cdot K_{fe} \cdot S_{cable}}{N \cdot p} + D_{strand}^2} - D_{strand}}{2} \quad (5)$$

For the cable used in the cos-theta Nb3Sn dipole magnets for VLHC [4-6] with  $S_{cable}=14.232 \times 1.8=25.6 \text{ mm}^2$ , the thickness of the strand coating is 8.6 microns. If the ferromagnetic material is a foil core – the cross-section area of the core must be equal to  $K_{fe} \cdot S_{cable}=0.03 \times 25.6=0.77 \text{ mm}^2$ . Thus, if the core width, for example, equals to the cable width\*, its thickness must be  $0.79/14.232=0.054 \text{ mm}$ .

Figure 2 shows the absolute sextupole field component induced by the magnetization of coil and by the ferromagnetic strips inside of the cable, and the resulting dependence without the yoke saturation effect. The strip width is equal to the cable width and its thickness is  $57.5 \text{ }\mu\text{m}$ . The magnetic properties of the iron strips were taken as for the HGQ iron yoke.

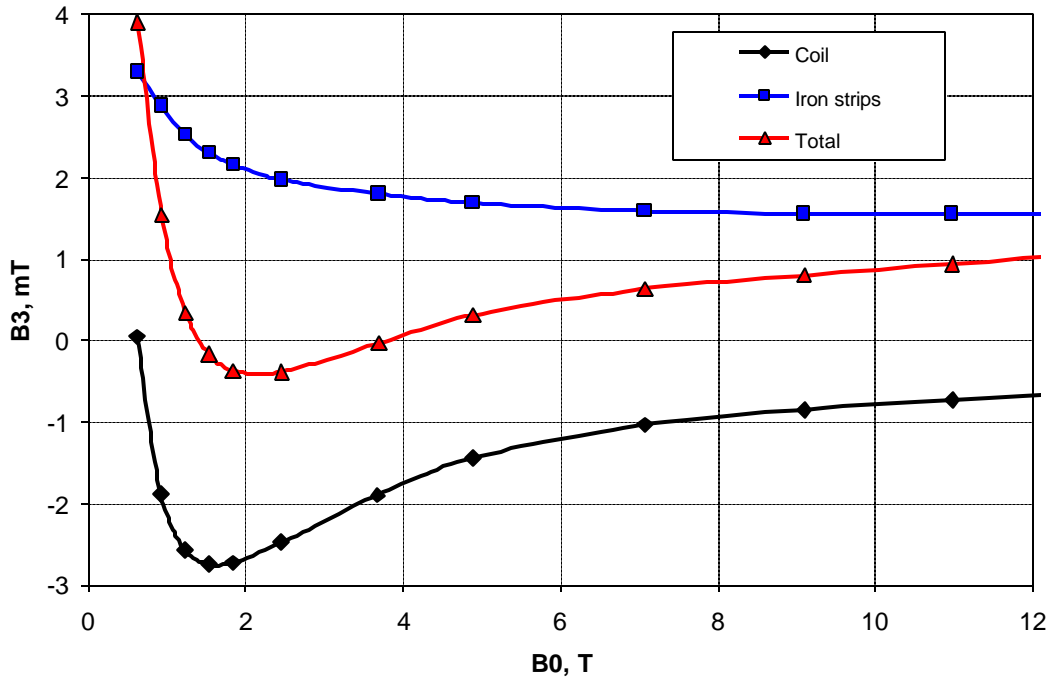


Figure 2: Absolute sextupole field component @ 1 cm radius produced by the persistent currents in the coil, ferromagnetic material in the coil, and their combination versus the bore field.

\* Real core width must be little bit smaller to allow strand transition from one layer to another one on the cable edges.

### 3. GEOMETRICAL AND PASSIVE CORRECTION

As one can see from Figure 2 there is a big overcompensation of sextupole components at high fields, which increases the required active corrector strength. In order to cancel the sextupole component within the operating field range without a passive correction one would need  $\sim 2.8 \text{ mT/cm}^2$  of the distributed active corrector strength, when in the case with passive correction one would need  $\sim 1.0 \text{ mT/cm}^2$  or only by factor of two smaller. Also, the presented case of passive correction requires the active corrector to work in the bipolar regime that is not well suitable mode for superconducting correctors. However, as it follows from Figure 2, the positive part of the corrected sextupole curve can be quite well approximated by the straight line. Then, if to remember that geometrical multipole errors in absolute units are the straight lines, increasing proportionally to the field, a compensation of linear part of the sextupole component at high fields could be done by introducing an appropriate artificial geometrical error in the coil.

Figure 3 shows the result of introduction the sextupole error ( $b_3 = -0.86$  units), which cancels the sextupole in the fields above 6 T. Thus, after additional geometrical correction the required active sextupole strength is reduced to  $0.6 \text{ mT/cm}^2$ . It is by factor of five smaller than in the case without any correction.

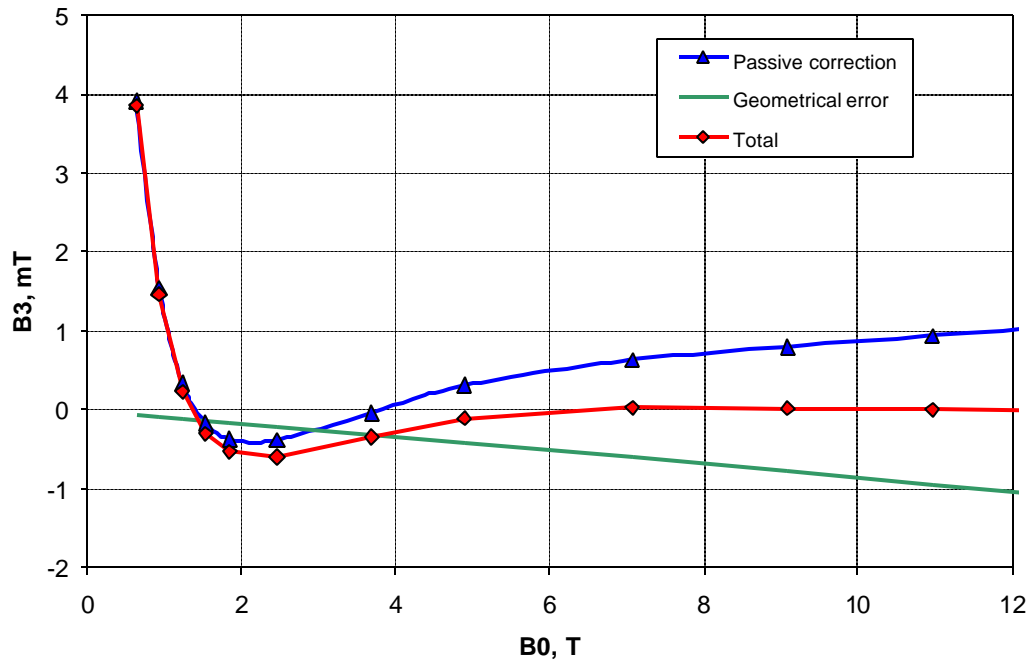


Figure 3: Combination of passive correction with geometry optimization.

The artificial geometrical error allows effective compensation of the sextupole component only at high fields. Its compensation effect at low fields is rather small as it is shown in Figure 4 where only a geometrical correction ( $b_3 = 0.66$ ) is used in order to cancel non-corrected sextupole at 11 T field.

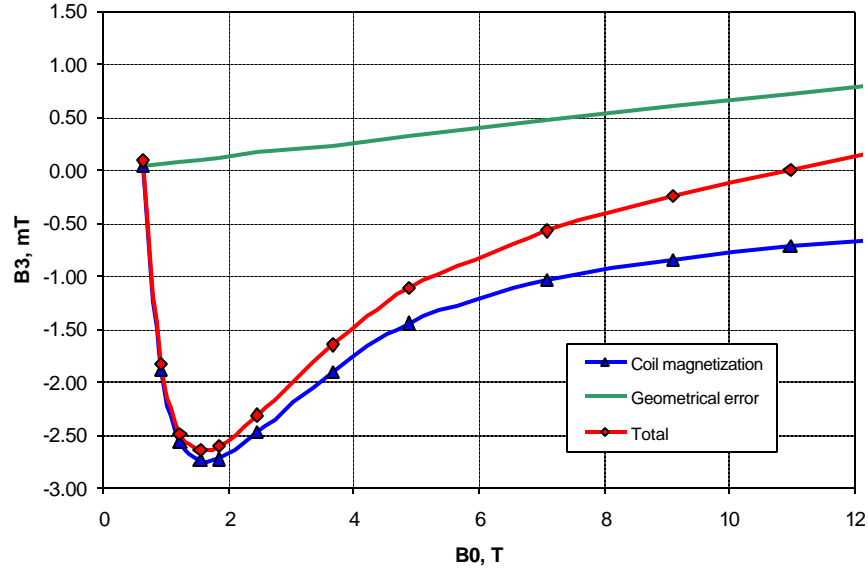


Figure 4: Correction of the magnetization sextupole by the geometrical component.

#### 4. CORRECTION OF COIL MAGNETIZATION EFFECT IN THE $\cos(\Theta)$ DIPOLE

The described above approach based on the combination of passive and geometrical correction schemes, has been applied for correction of the coil magnetization effect in high field Nb3Sn dipoles for VLHC [3-6]. Iron yoke saturation effect was also included. Several cases with different position of the correcting material and different material parameters were simulated using OPERA 2D code. In the first case, thin ferromagnetic strips were placed between all the cables. In the second case, the ferromagnetic strip was placed inside the cable and had a width equals to the cable width. In the third case the strip width was only half of the cable width. Two possible positions of the correcting ferromagnetic strips inside the magnet coil are shown in Figure 5. The thickness of the strips was optimized to eliminate the sextupole component at the reference field of 3.7 T.

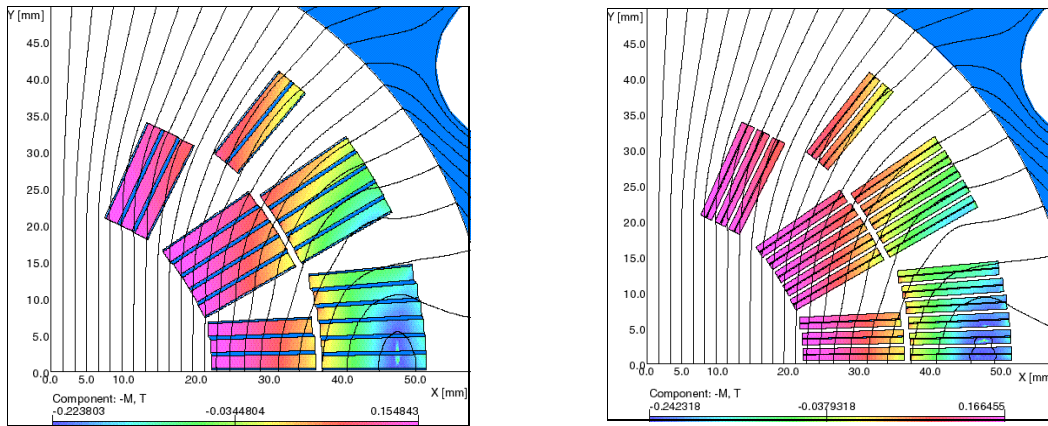


Figure 5: Simulation of strips inside the coil at  $B_0 = 1.2$  T:  
left – strips between the cables; right – strips inside the cables.

Figures 6 and 7 show normalized sextupole and decapole field components versus the bore field for all the above-mentioned cases and for the “strips on the pipe” type corrector [2]. As one can see, the strips placed inside the coil provide similar correction effect as the strips placed inside the magnet bore for the magnetization sextupole and less effect for the decapole.

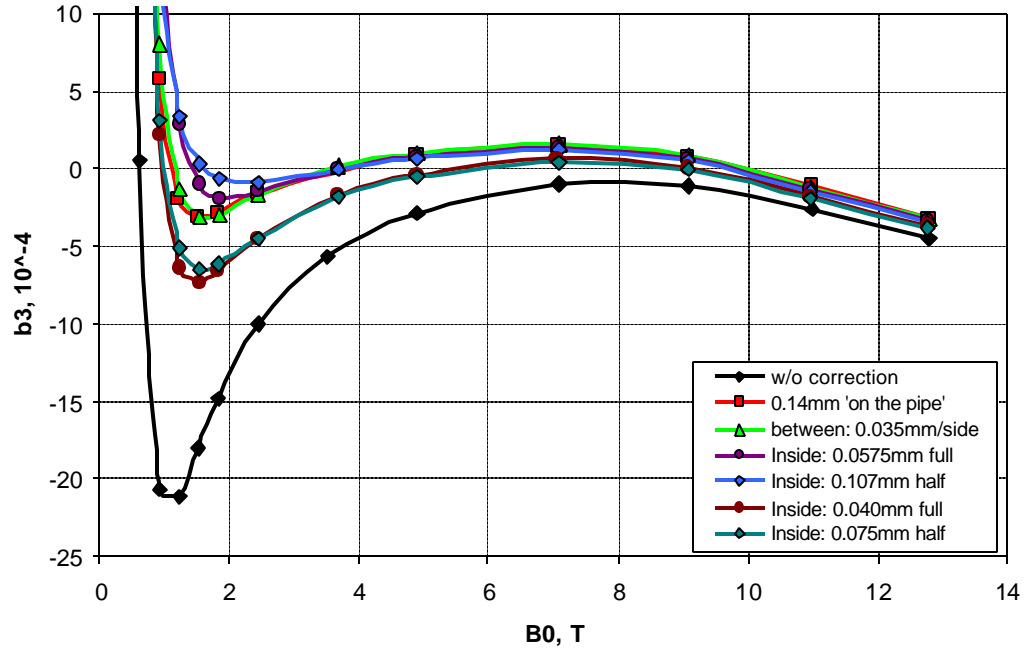


Figure 6: Sextupole field component versus the bore field.

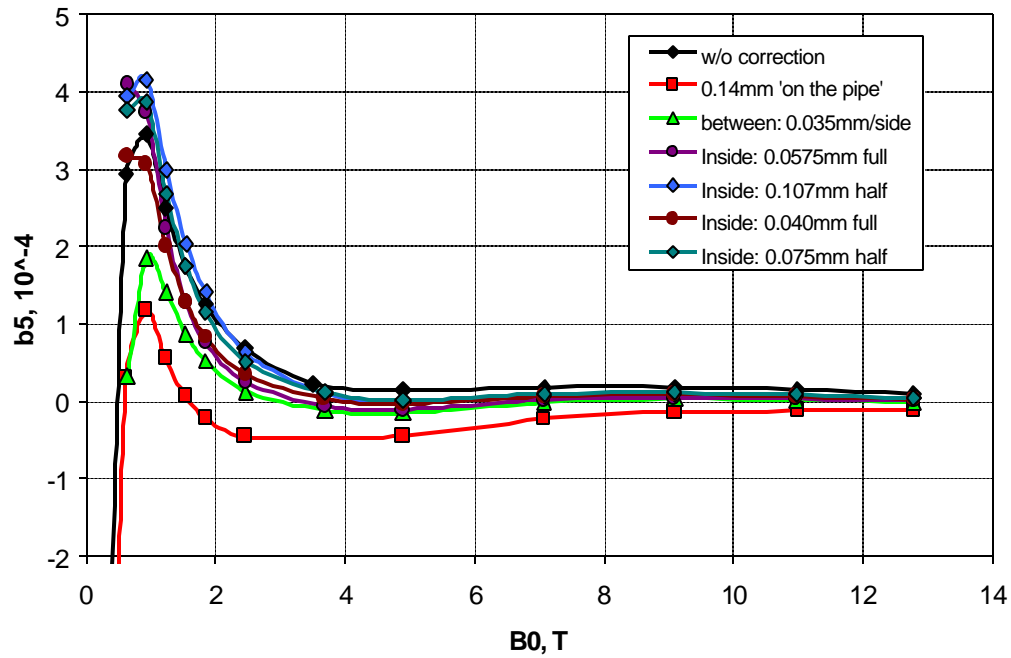


Figure 7: Decapole field component versus the bore field.

Table 1 and 2 summarize high order multipoles as a function of the current in the coil and the bore field for the ferromagnetic strips, placed inside the coil, and for the “strips on the pipe” type corrector.

Table 1: High order multipoles w/o correction and corrected by strips on the pipe.

I, kA	B <sub>0</sub> , T	No correction			“Strips on the pipe”		
		b7	b9	b11	b7	b9	b11
1	0.62	-0.39	0.07	0.13	0.24	-0.26	-0.23
2	1.23	-0.60	0.06	0.14	-0.08	-0.21	-0.03
3	1.84	-0.35	-0.01	0.12	0.09	-0.24	0.03
8	4.88	-0.05	-0.08	0.10	0.15	-0.21	0.08
12	7.07	-0.02	-0.09	0.10	0.12	-0.18	0.09
20	11.0	-0.01	-0.10	0.11	0.08	-0.16	0.10

Table 2: High order multipoles corrected by strips inside the coil.

I, kA	B <sub>0</sub> , T	Between cables			Full inside (57.5 $\mu$ m)			Half inside (75 $\mu$ m)		
		b7	b9	b11	b7	b9	b11	b7	b9	b11
1	0.62	0.31	-0.07	0.19	0.68	0.14	0.26	0.13	0.12	0.25
2	1.23	-0.31	-0.03	0.11	-0.26	0.00	0.14	-0.30	0.05	0.16
3	1.84	-0.15	-0.07	0.10	-0.18	-0.06	0.11	-0.18	-0.02	0.12
8	4.88	0.03	-0.10	0.10	0.01	-0.09	0.10	-0.02	-0.08	0.10
12	7.07	0.04	-0.10	0.10	0.02	-0.09	0.11	0.00	-0.09	0.11
20	11.0	0.02	-0.10	0.10	0.02	-0.10	0.10	0.00	-0.10	0.11

In order to calculate sensitivity of field harmonics to the strip thickness, one can use the plots shown in Figure 6 and 7. As one can see, sensitivity of the sextupole is about 0.5 unit/ $\mu$ m at low field, sensitivity of the decapole component practically is even smaller.

Two cases with non-central strip positions were also considered in order to check sensitivity to the possible strip displacement during cable manufacturing. In both cases the strip width was 0.75 of the cable width. First, the strip was aligned to the inner cable edge and then to the outer cable edge. Thus, strip displacement between the inner and the outer cable edge was 0.25 of the cable width or 3.5 mm. The variation of the sextupole and decapole field components between these two cases at 1.2 T was 6.9 and 0.7 units respectively. Based on that, the strip displacement by  $\pm 0.5$  mm from its designed position gives  $\pm 1$  unit of sextupole deviation.

## 5. CORRECTION OF COIL MAGNETIZATION EFFECT IN THE COMMON-COIL DIPOLE

The proposed technique of the persistent current correction was also implemented in one of the common-coil magnet designs [3]. In order to simplify the finite-element model, only the case with strips between cables was considered, since it had shown results close to the other cases. The worst case when both inner and outer coils are made from Nb<sub>3</sub>Sn conductor with copper to superconductor ratio of 0.85 was considered.

Figure 8 shows two cases of the two-layer common coil dipole with magnetization and flux lines at the bore field of 1.14 T.

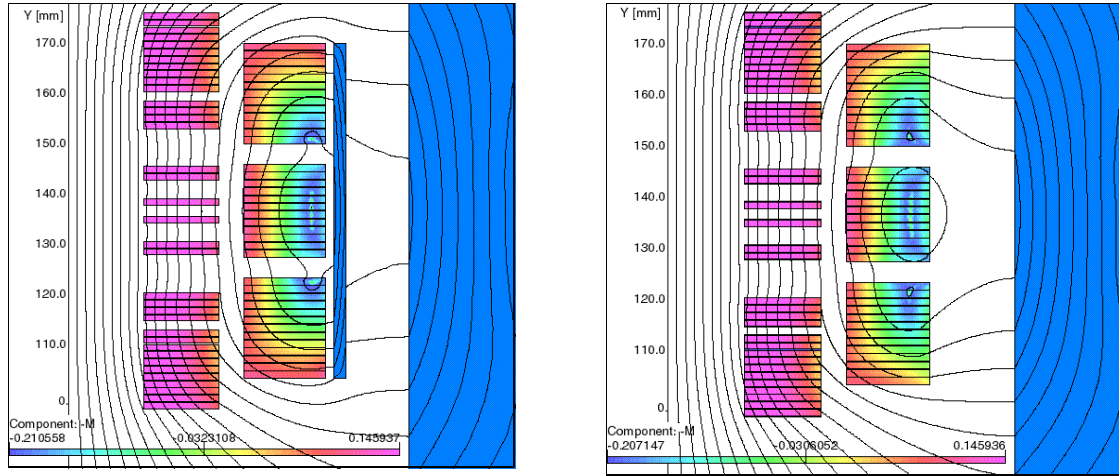


Figure 8: Simulation of the persistent current correction at  $B_0=1.14$  T: left –correction by 2.5mm iron wall; right – strips between the cables.

Figures 9 and 10 show results of comparison of the persistent current correction by the iron wall outside the coil [3] and correction by the strips placed between turns. Table 3 summarizes the high order multipoles for the considered cases.

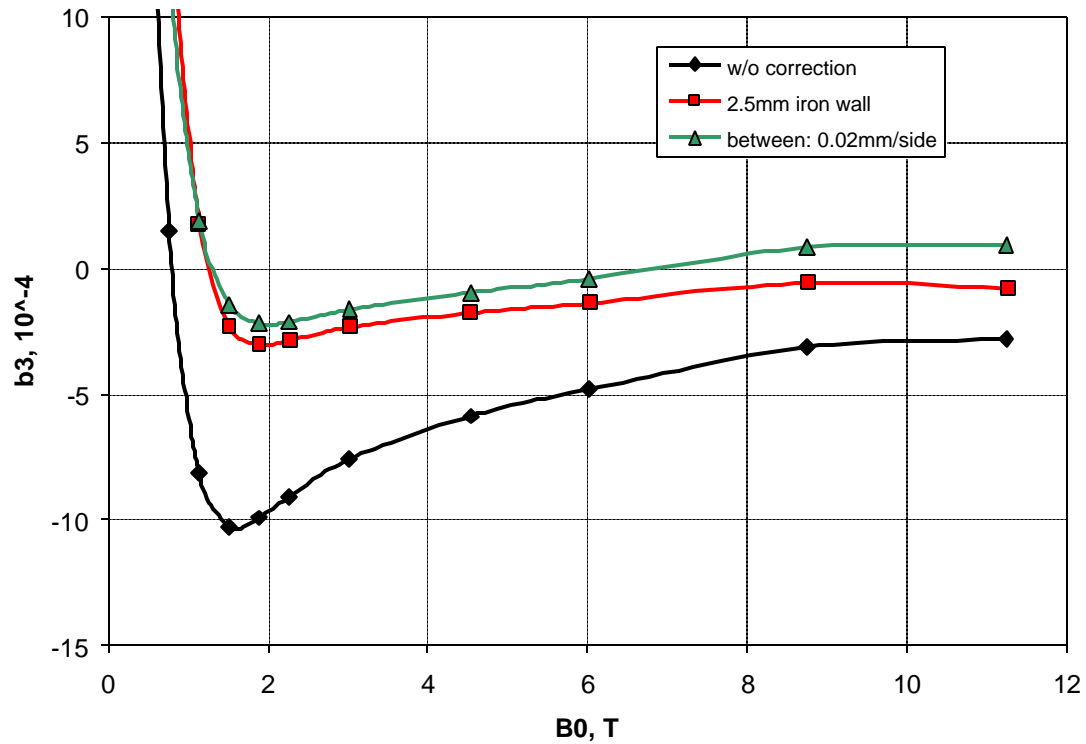


Figure 9: Sextupole field component versus the bore field.



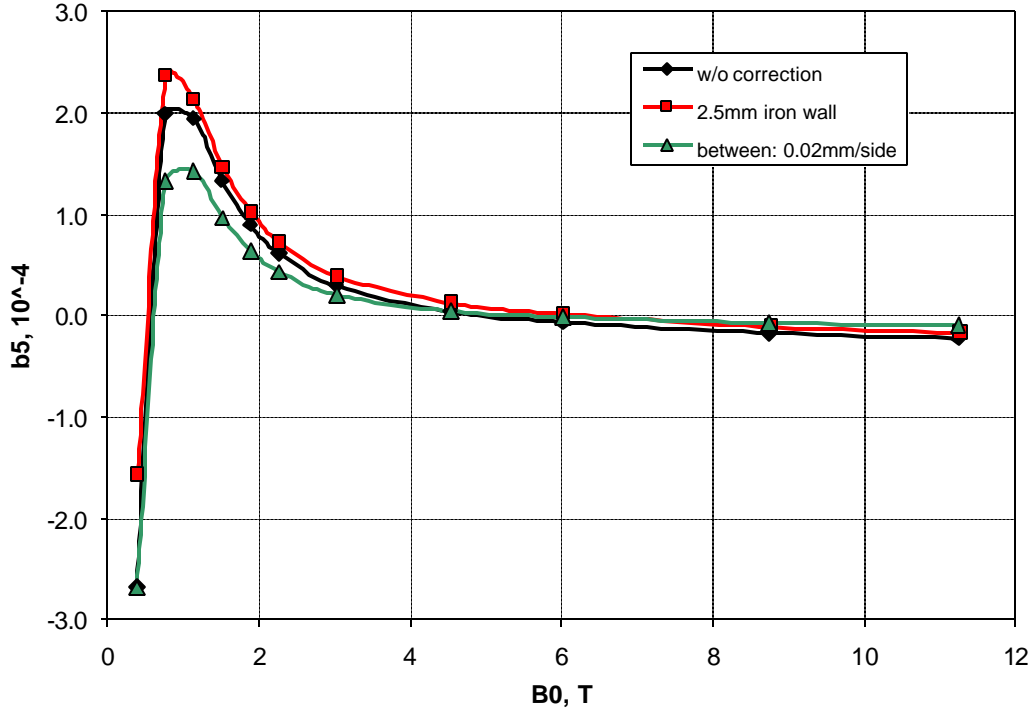


Figure 10: Decapole field component versus the bore field.

Table 3: High order multipoles for different correction schemes.

I, kA	$B_0$ , T	No correction			Iron wall			Strip between cables		
		b7	b9	b11	b7	b9	b11	b7	b9	b11
1	0.77	-0.39	-0.29	0.66	-0.39	-0.29	0.69	0.04	-0.28	0.49
2	1.52	-0.03	-0.34	0.46	-0.02	-0.34	0.46	0.20	-0.32	0.35
3	2.28	0.16	-0.34	0.34	0.17	-0.34	0.34	0.32	-0.33	0.27
6	4.53	0.31	-0.35	0.25	0.32	-0.35	0.25	0.38	-0.34	0.21
12	8.74	0.35	-0.36	0.24	0.36	-0.36	0.24	0.40	-0.36	0.22
16	11.2	0.38	-0.38	0.24	0.37	-0.37	0.24	0.41	-0.37	0.23

The value of magnetization sextupole at low field in the common coil dipole is by factor of two smaller then for the cos-theta dipole. It can be explained by small turn density in the midplane area close to the bore. As in the case of cos-theta magnets, either iron wall outside the coil or 20 micron strips (40 micron core) inside the coil allow reducing the sextupole component in the common coil magnet design to the acceptable level. One can notice also that the correction effect on the decapole component in case of magnetization compensation is small or even slightly negative.

## 6. CONCLUSIONS

The method of compensation of coil magnetization effect using distributed in the coil iron strips or iron core in the cable allows effectively eliminate the induced field sextupole with small effect on the decapole at low fields while keeping the higher order

multipoles at an acceptable level. Taking an advantage of placing strip inside the cable, one can combine together correction of the persistent current effect and reduction of the interstrand coupling currents by choosing the strip material with high resistance.

The approach with strips between the cables may be easily implemented in the common-coil magnet design due to their plain racetrack coils. In case of the ferromagnetic strip inside or between the cables, the exact designed positioning of the corrector achieves automatically during coil winding that eliminates alignment and calibrating procedures and may be attractive for the magnet mass production.

It was also shown that passive correction of the coil magnetization effect becomes very efficient in combination with coil geometry optimization. This statement is valid for all types of passive correction of coil magnetization effect with ferromagnetic strips.

Proposed correction method is applicable not only for accelerator magnets, but to any other superconducting magnets (solenoids) when reduction of the superconductor magnetization effect is required.

## REFERENCES

1. V.V. Kashikhin and A.V. Zlobin, "Correction of Coil Magnetization Effect in Nb<sub>3</sub>Sn High Field Dipole Magnet Using Thin Iron Strips", Fermilab, TD-99-048, October 15, 1999.
2. V.V. Kashikhin and A.V. Zlobin, "Comparison of Correcting Capability of Passive Correctors Based on a Thin Pipe and Thin Strips", Fermilab, TD-99-049, October 15, 1999.
3. P. Bauer, G. Sabbi, N. Andreev, E. Barzi, "2nd Iteration Magnetic Design for the First FNAL Common Coil Nb<sub>3</sub>Sn Dipole Model", Fermilab, TD-00-028, April 13, 2000.
4. V.V. Kashikhin and A.V. Zlobin, "Conceptual Magnetic Design of the Fermilab 2-in-1 Nb<sub>3</sub>Sn Dipole Magnet for VLHC", Fermilab, TD-00-008, February 4, 2000.
5. V.V. Kashikhin and A.V. Zlobin, "Iron Yoke Optimization in Double Aperture Nb<sub>3</sub>Sn Dipole Magnet for VLHC", Fermilab, TD-00-009, February 4, 2000.
6. V.V. Kashikhin and A.V. Zlobin, "Compensation of Quadrupole Field Component in the VLHC Double Aperture Nb<sub>3</sub>Sn Dipole Magnet with Warm Iron Yoke", Fermilab, TD-00-036, May 25, 2000.